

# Gene Transfer to Rabbit Retina with Electron Avalanche Transfection

Thomas W. Chalberg,<sup>1</sup> Alexander Vankov,<sup>2,3</sup> Fanni E. Molnar,<sup>2</sup> Alexander F. Butterwick,<sup>2,3</sup> Philip Huie,<sup>2,3</sup> Michele P. Calos,<sup>1</sup> and Daniel V. Palanker<sup>2,3</sup>

**PURPOSE.** Nonviral gene therapy represents a promising treatment for retinal diseases, given clinically acceptable methods for efficient gene transfer. Electroporation is widely used for transfection, but causes significant collateral damage and a high rate of cell death, especially in applications in situ. This study was conducted in the interest of developing efficient and less toxic forms of gene transfer for the eye.

**METHODS.** A novel method for nonviral DNA transfer, called electron avalanche transfection, was used that involves microsecond electric plasma-mediated discharges applied via microelectrode array. This transfection method, which produces synchronized pulses of mechanical stress and high electric field, was first applied to chorioallantoic membrane as a model system and then to rabbit RPE in vivo. Gene transfer was measured by using luciferase bioluminescence and in vivo fluorescent fundus photography. Safety was evaluated by performing electroretinograms and histology.

**RESULTS.** In chorioallantoic membrane, electron avalanche transfection was ~10,000-fold more efficient and produced less tissue damage than conventional electroporation. Also demonstrated was efficient plasmid DNA transfer to the rabbit retina after subretinal DNA injection and transscleral electron avalanche transfection. Electroretinograms and histology showed no evidence of damage from the procedure.

**CONCLUSIONS.** Electron avalanche transfection is a powerful new technology for safe DNA delivery that has great promise as a nonviral system of gene transfer. (*Invest Ophthalmol Vis Sci*. 2006;47:4083–4090) DOI:10.1167/iovs.06-0092

Retinal degenerative diseases, such as age-related macular degeneration and a family of diseases known as retinitis pigmentosa, have several genetic causes (summarized at RetNet: <http://www.sph.uth.tmc.edu/retnet/> provided in the public domain by the University of Texas Houston Health Science Center, Houston, TX) that affect the photoreceptor cells or the retinal pigment epithelial (RPE) layer that supports them. Gene therapy represents potentially a powerful approach to treating retinal diseases.<sup>1</sup> Indeed, investigators in several studies have

used viral vectors for gene delivery to photoreceptor cells<sup>2–4</sup> and RPE cells.<sup>5–7</sup>

Despite these successes, viral vectors suffer from many drawbacks: they can be immunogenic and toxic and, most notably for adenoassociated virus, have limited carrying capacity.<sup>8</sup> Moreover, viral vectors are difficult and expensive to manufacture, and randomly integrating viruses have led to insertional mutagenesis.<sup>9</sup> Consequently, interest in nonviral gene delivery has grown. Chemical methods, such as liposomes, are often inefficient and toxic to cells.<sup>10</sup> Electroporation is effective for nearly all cell types and has become widely adopted as the method of choice for hard-to-transfect cells.<sup>11</sup> Electroporation is useful both for large molecules such as plasmid DNA and small molecules, but the mechanism of electrotransfer seems to be different. Whereas very short (microsecond) pulses are sufficient for small molecule delivery, efficient DNA delivery typically requires longer (20–50 ms) pulses.<sup>11</sup> The major disadvantage of electroporation is the high rate of cell death, which is considered an unavoidable consequence of the technology itself.<sup>12</sup> This limitation is especially significant for transfection of tissues in situ. Damage may occur by loss of cytoplasmic materials from the cell due to prolonged permeabilization of the cell membrane and also as a result of thermal damage.<sup>13,14</sup> Amaxa Biosystems (Cologne, Germany) offers proprietary technology for efficient transfection, particularly for primary cells. These methods are available for a limited number of cell types and still lead to a high rate of cell death.<sup>15</sup>

Sonoporation (the use of ultrasound) has recently been demonstrated for DNA,<sup>12,16</sup> as well as for small molecules,<sup>17–20</sup> and is thought to affect cellular membranes through a mechanism of acoustic cavitation involving the creation and collapse of gas bubbles.<sup>21</sup> Optimized in a muscle cell line, sonoporation has been reported to be relatively inefficient (transfection of ~2%–4%) and somewhat toxic (viability of ~60%–80%).<sup>12</sup> Some models indicate that mechanical stress can also cause formation of pores in cellular membranes.<sup>22</sup>

In this investigation, we sought to optimize electroporation parameters for gene transfer to RPE in a larger animal model, to overcome the limitations of conventional electroporation seen in our previous study in rats.<sup>23</sup> In that study, which used corneal placement of conventional electrodes, much of the ocular damage that was observed, such as corneal wounds and cataracts, was associated with the anterior structures of the eye. Our current approach used the electrodes placed behind the eye, thus keeping them away from the sensitive anterior structures and closer to the retinal cells that were the targets of DNA transfer (Fig. 1a). In this design, the electrodes are separated from the targeted RPE cells by the sclera and choroid. Photoreceptor cells are at a greater distance over the area of the induced retinal detachment associated with subretinal injection of DNA. We began with a model system, chorioallantoic membrane (CAM), and moved to rabbits as a model organism, which have large eyes and allow for more elaborate surgical techniques that are more readily translated to the clinic. We developed a new technology for nonviral gene transfer that uses a combination of high electric field and mechanical stress,

From the Departments of <sup>1</sup>Genetics and <sup>2</sup>Ophthalmology, Stanford University School of Medicine, and the <sup>3</sup>Hansen Experimental Physics Laboratory, Stanford University, Stanford, California.

Supported by National Heart, Lung, and Blood Institute Grant HL68112 and National Eye Institute Grants EY16702 (MPC) and EY01288 (DVP), Whitaker Foundation Grant RG030042 (DVP), and Stanford MFEL Program grant AFOSR (DVP). TWC was a Howard Hughes Medical Institute Predoctoral Fellow.

Submitted for publication January 29, 2006; revised March 26, 2006; accepted June 26, 2006.

Disclosure: T.W. Chalberg, P; A. Vankov, P; F.E. Molnar, None; A.F. Butterwick, None; P. Huie, P; M.P. Calos, None; D.V. Palanker, P

The publication costs of this article were defrayed in part by page charge payment. This article must therefore be marked "advertisement" in accordance with 18 U.S.C. §1734 solely to indicate this fact.

Corresponding author: Daniel V. Palanker, Stanford University, Hansen Experimental Physics Laboratory, 445 Via Palou, Stanford, CA 94305-4085; palanker@stanford.edu.

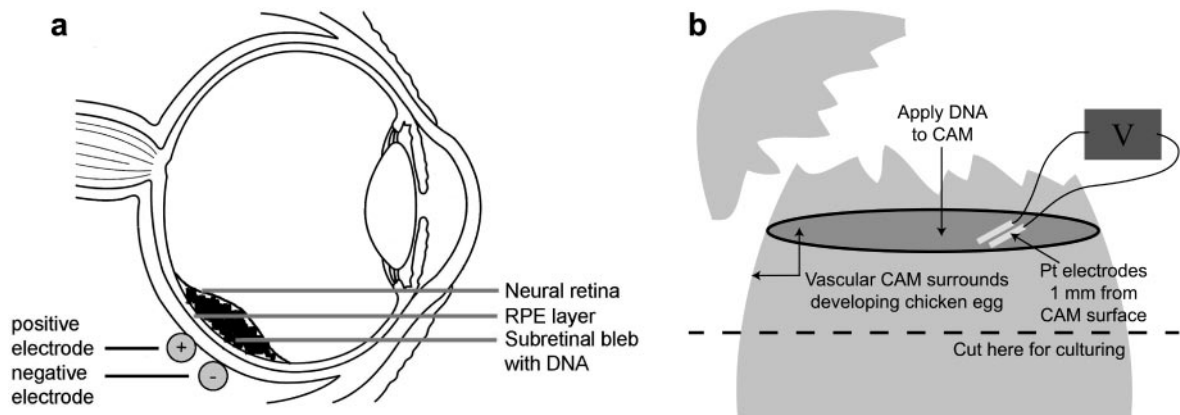


**FIGURE 1.** Schematic diagram of DNA transfer to retinal cells in vivo and in a model system. **(a)** For delivery to retinal cells in vivo, DNA is first injected into the subretinal space. Positive and negative electrodes are placed behind the eye, separated from the targeted RPE cells by the thickness of the sclera. Eye image is courtesy of the National Eye Institute, National Institutes of Health. **(b)** CAM from developing chicken eggs is a model system for DNA transfer to RPE. DNA is pipetted directly onto the CAM, and platinum electrodes are placed 0.2 mm from the target tissue.

called electron avalanche transfection. We evaluated the efficacy and safety of this technique in the rabbit retina.

## METHODS

### Plasmid Constructs

The luciferase expression plasmid pNBL2<sup>24</sup> has been described. The pMax vector was obtained from Amaxa Biosystems.

### Electroporation Protocols

For conventional electroporation, a pair of platinum electrodes was constructed having a width of 1 mm and length of 4 mm, and separated by 4 mm. A variety of settings was used in initial electroporation experiments. Optimized parameters involved a high-voltage square-wave pulse lasting 250  $\mu$ s at +150 V, followed immediately by a low-voltage square-wave pulse lasting 5 ms at -5 V. Fifty such cycles were applied at 1 Hz. These parameters were used in subsequent experiments with CAM and rabbits. To apply tensile stress, a 0.2-mm agarose gel was used to separate electrodes from the CAM. By pushing down on the agarose gel slice, the CAM layer was stretched by ~5%. Application of ultrasound used the settings 2.4 W/cm<sup>2</sup> 60-kHz ultrasound for 50 seconds (Transducer US 15CB; Nakanishi Inc., Kanuma, Japan).

For electron avalanche gene transfer, biphasic pulses of 250  $\mu$ s per phase were applied. Experiments on CAM used a single 100- $\mu$ m microelectrode 1 mm in length and a range of voltage settings from  $\pm$ 250 to  $\pm$ 600 V. For rabbit RPE experiments, two probes were constructed. The first had an array of three horizontal microelectrodes 50  $\mu$ m in diameter and 1.5 mm in length, surrounded by a return electrode. The second contained nine microelectrodes 50  $\mu$ m in diameter that protruded above the plane of the probe by 100  $\mu$ m. In both cases, the face of the probe containing the microelectrode array was 3  $\times$  3 mm. Both probes also contained an optical fiber illuminated with a xenon lamp (Ophthalmic Technologies, Inc., Toronto, ON, Canada) to facilitate localization of the probe under the bleb. In rabbit experiments  $\pm$ 250 V was used, and five pulses were applied at each location, with 5 to 15 locations treated in each eye.

### CAM Gene Transfer and Culture

Fertilized chicken eggs (California Golden Eggs, Sacramento, CA) were incubated under development conditions until days 9 to 13. The shell and shell membrane were removed to expose the CAM surface, 100  $\mu$ g of pNBL2 plasmid DNA encoding the luciferase gene in 1.1 mL PBS were pipetted onto the membrane, electrodes were placed in the DNA solution ~0.2 mm from the CAM surface, and pulses were applied. To

culture the tissue, the shell, shell membrane, and CAM were carefully cut with scissors ~1 cm below the first cut, so that the treated area remained intact and the eggshell ring formed a scaffold to support the CAM. The tissue was washed twice for 15 minutes in 2 $\times$  antibiotic-antimycotic (Invitrogen, Carlsbad, CA), rinsed with PBS (Invitrogen), and cultured in Dulbecco's modified Eagle's medium (Invitrogen) supplemented with 10% fetal bovine serum.

### Animal Studies

Initial experiments measuring luciferase activity were performed with 1.8- to 2.0-kg Dutch Belted rabbits, and 3.5- to 4.5-kg New Zealand White rabbits (Myrtle's Rabbitry, Thompson Station, TN) were used in all subsequent experiments. All experimental protocols were conducted in accordance with the ARVO Statement for the Use of Animals in Ophthalmic and Vision Research and were approved by the Administrative Panel on Laboratory Animal Care at Stanford University.

### Subretinal Injection and Electroporation In Vivo

Animals were anesthetized with 40 mg/kg ketamine (Vedco, St. Joseph, MO), 5 mg/kg xylazine (Vedco), and 0.02 mg/kg glycopyrrolate (Baxter, Deerfield, IL). Atropine 1% (Alcon Laboratories, Fort Worth, TX), phenylephrine 2.5% (Alcon), tetracaine 0.5% (Alcon), and methylcellulose gel 2.5% (Akorn, Buffalo Grove, IL) were applied to the eyes. A corneoscleral limbus-based conjunctival peritomy was performed to allow electrode access to the back of the eye, and space was opened by separating, blunt-tipped tenotomy scissors. A 25-gauge trocar-cannula (Alcon) was pushed through the sclera 3.5 mm from the corneoscleral limbus at a steep angle to avoid the lens, and the trocar was removed leaving the cannula in place.

For the subretinal injection, a 1-mL tuberculin syringe (BD Biosciences, Franklin Lakes, NJ) connected to 10 cm of tubing ending in a 30-gauge needle (BD Biosciences) that had been blunted and polished was loaded with DNA and the air bubbles removed. The needle was guided through the cannula until it was just above the retina. A pulse of DNA was injected, consisting of 50 to 100  $\mu$ L of 1  $\mu$ g/ $\mu$ L DNA in physiologic saline solution (PSS) (Balanced Salt Solution, BSS; Alcon Laboratories), forming a subretinal bleb. Electrodes were placed through the peritomy. The lamp on the electrode was used to align probe directly under the bleb and five pulses were applied. The electrodes were moved slightly, and the next set of pulses were applied to cover the bleb. The sclerotomy and peritomy were closed with 7-0 Vicryl sutures (Ethicon, Somerville, NJ). After surgery, animals received atropine eye drops, subconjunctival triamcinolone (Bristol-Myers Squibb, New York, NY), and corneal application of ointment

containing bacitracin zinc (500 U/g) and polymixin B sulfate (10,000 U/g; Akorn).

## Evaluation of Gene Transfer

Bioluminescence imaging was performed *in vitro* for both CAM and for freshly enucleated rabbit eyecups 24 hours after gene transfer. The posterior eyecup was prepared, and the neural retina was left in place. Drops of luciferin substrate (30 mg/mL) were applied to the tissue. After 10 minutes, bioluminescence was measured (IVIS 200; Xenogen, Alameda, CA). After the initial measurement, the neural retina was removed, luciferin was reapplied directly to the RPE, and bioluminescence imaging was repeated.

For *in vivo* fluorescence imaging, animals were anesthetized and their pupils dilated as described earlier. A surgical microscope equipped with a 465- to 495-nm blue excitation filter and 518- to 557-nm green emission filter was connected to a digital camera (Retiga 1300; QImaging, Burnaby, BC, Canada). The retina was photographed (Mini Quad VIT lens; Volk Optical, Mentor, OH).

## Electroretinograms

Animals were anesthetized and their eyes dilated as described earlier. Electrodes were made by fixing a silver reference electrode to a standard JET electrode (LKC Technologies Inc., Gaithersburg, MD). ERGs were measured in response to a flash from bilaterally placed full-field stimulators (model 1621I; Grass-Telefactor, West Warwick, RI). Stimulation light intensity was measured as  $1.5 \text{ cd} \cdot \text{s}/\text{m}^2$ . Animals were placed in a Faraday cage, and light adaptation measurements were taken after 2 minutes of full-field exposure to LEDs of  $20 \text{ cd}/\text{m}^2$  and averaged over 60 flashes at 1 Hz. After 45 minutes of dark adaptation, two recordings were taken 45 seconds apart, and the response was averaged over the two recordings. Recordings were filtered and amplified (SR560 amplifier; Stanford Research Systems, Sunnyvale, CA) and recorded on a digital oscilloscope (TDS 3034; Tektronix Inc., Beaverton, OR). Data were analyzed (MatLab; Mathworks Inc, Natick, MA), smoothed with the spline function, and adjusted to agree 7 ms after the stimulus to negate the stimulus artifact. Data were evaluated by comparing the a- and b-wave amplitudes in treated and untreated eyes.

## Histology

Animals were euthanized by intravenous injection (85 mg/kg Beuthanasia-D; Schering-Plough Animal Health, Omaha, NE). Eyeballs were enucleated and histology was prepared as described.<sup>25</sup> Briefly, eyes were placed immediately into fixative containing 2.5% glutaraldehyde and 1% paraformaldehyde in Sorenson's phosphate buffer containing 1.5% sucrose and 1 mM  $\text{MgSO}_4$  (pH 7.4). The tissue was fixed overnight and washed with 0.1 M Sorenson's phosphate buffer containing 1.5% sucrose, dehydrated in a series of methanol and acetone, and embedded in resin (Eponate 12/DMP-30; Ted Pella, Redding, CA). One-micrometer sections were cut with a microtome (OMU-3; Reichert, Vienna, Austria) and stained with toluidine blue for light microscopy.

Frozen sections were prepared for fluorescence microscopy as described.<sup>26</sup> Tissue was fixed immediately in freshly prepared 4% paraformaldehyde in Sorenson's phosphate buffer (pH 7.4), for 24 hours. The tissue was cryoprotected with 30% sucrose in Sorenson's phosphate buffer, embedded (Optimal Cutting Temperature compound; Sakura Finetechnical Co., Tokyo, Japan), and sectioned with a cryostat (Ultracut E; Leica, Deerfield, IL). Fluorescence microscopy was performed on frozen sections (Axioplan 2 fluorescence microscope; Carl Zeiss Meditec, Dublin, CA), with an autofluorescence reducing green fluorescent protein (GFP) filter cube (Chroma Technology, Brattleboro, VT) and the microscope software (AxioVision; Carl Zeiss Meditec).

## RESULTS

### Optimization of Electroporation in CAM

Because electroporation protocols vary for different tissues, our initial experiments were conducted to achieve a better understanding and optimization of pulse parameters for RPE transfection. Electroporation protocols that have been optimized for other tissues such as muscle<sup>11</sup> have used a train of pulses for DNA delivery, each pulse having a short (microsecond), high-voltage phase followed by a long (millisecond), low-voltage phase. Optimization must account for many parameters, including electrode size and spacing, the number of pulses, short- and long-pulse durations and amplitudes, and polarity of the two pulses.

We started optimization with a model tissue, the CAM from the developing chicken egg, which has been used to model retinal tissue for surgical techniques.<sup>27,28</sup> CAM is a live, readily available, and inexpensive tissue. Its epithelial layer is uniform and has high resistance, making it a good model for RPE. In this model system, 100  $\mu\text{g}$  of pNBL2 plasmid DNA encoding the luciferase gene was pipetted onto the CAM, and pulses were applied (Fig. 1b). The tissue was then cultured and assayed for luciferase bioluminescence.

These optimization experiments demonstrated the best DNA transfer with the least amount of damage when multiple pulses were applied and when a short, high-voltage pulse was followed by a long, low-voltage pulse. These results are consistent with previous studies optimizing DNA transfer to muscle.<sup>11</sup> Specifically, the optimized parameters were a 250- $\mu\text{s}$ , 150 V-phase, followed by a 5-ms, 5-V phase in the same polarity. Optimal results were achieved with 50 cycles applied at 1 Hz. When electrodes were placed in contact with CAM, luciferase expression levels were  $\sim 10^6$  photons/s. At distances of 0.2 mm, however, much lower levels of signal ( $10^4$  photons/s) were observed in each treated area (Fig. 2a). We reasoned that the higher expression with direct electrode contact could be either due to the target cells experiencing a higher electric field due to the closer proximity of the electrodes or to the pressure of the electrodes on the CAM surface causing the CAM to stretch, which contributed to DNA transfer. To test whether tissue stretching affects DNA transfer, we placed a 0.2-mm layer of 1% agarose gel between the CAM and the electrodes. The resistance of the agarose gel was similar to that of saline and the sclera-choroid. Slight pressure was applied to the electrodes to stretch the CAM by  $\sim 5\%$ . Electroporation with these settings yielded luciferase expression  $\sim 20$ -fold higher than at the same distance but without pressure (Fig. 2b).

We next asked whether another source of mechanical stress, ultrasound, could be used in combination with electroporation to enhance DNA transfer. Application of 2.4-W/ $\text{cm}^2$  and 60-kHz ultrasound for 50 seconds, a regimen similar to that used to transfect a muscle cell line,<sup>12</sup> led to luciferase signal levels lower than  $10^4$  photons/s (data not shown). In combination, however, ultrasound and electroporation yielded luciferase expression more than  $10^7$  photons/s,  $\sim 1000$ -fold above electroporation alone (Fig. 2b), suggesting that sources of mechanical stress in combination with high electric field could enhance the efficiency of DNA transfer.

### Electron Avalanche Transfection in CAM

When sufficiently high voltage is applied, a mechanical stress wave synchronized with a pulse of electric current can be produced by the electric discharge itself.<sup>28</sup> This occurs through rapid vaporization of conductive medium with a short (microseconds) pulse of current. Fast expansion and collapse of the transient cavitation bubble produces stress and tensile waves in the surrounding medium.<sup>29</sup> When the vapor bubble is

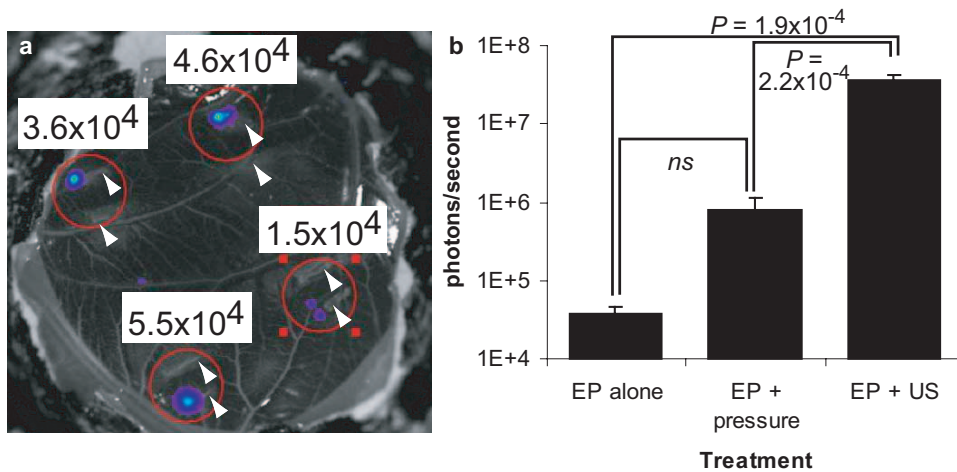


**FIGURE 2.** Optimization of electroporation in CAM. (a) CAM was assayed for luciferase expression (in photons/second) 24 hours after DNA transfer with four spots of noncontact electroporation under optimized settings. Damage from the electrodes caused obvious discoloration of the membrane (arrowheads). (b) Luciferase expression levels after electroporation alone (values from A), electroporation with mechanical stress, and electroporation with ultrasound. ANOVA statistical analysis showed that differences between groups were significant ( $P = 8.03 \times 10^{-5}$ ). Pair-wise *t*-tests with Bonferroni correction were then performed. Probabilities are as indicated;  $n = 4$  for each group.

formed, however, it disconnects the electrode from the conductive physiological medium, thus terminating the pulse of electric current. Conductivity can be restored by ionizing the vapor cavity, which can be achieved at sufficiently high voltage. This phenomenon has been used for tissue fragmentation and dissection.<sup>28,30,31</sup> We hypothesized that a similar regimen, in which high voltage is used as a source of both the high electric field and mechanical stress, would achieve efficient DNA transfer (Fig. 3a). This hypothesis was tested by using CAM in a protocol similar to that used for the conventional electroporation experiments. Using a 50- $\mu\text{m}$  wire microelectrode 1 mm in length, we applied a series of symmetric biphasic pulses, each phase being 250  $\mu\text{s}$  in duration and 600 V in amplitude. The microelectrode was scanned over a 4-mm<sup>2</sup> area, and approximately 50 pulses were applied. The resultant luciferase expression was  $\sim 10^9$  photons/s, 10,000-fold higher than levels seen with conventional electroporation alone (Fig. 3b). Highlighting the role of the plasma-mediated electric discharge, we named this novel technique electron avalanche-mediated transfection, or, for simplicity, the avalanche method.

### Electron Avalanche-Mediated Transfection in Rabbit Retina and RPE

Having observed efficient DNA delivery in a model tissue with electroporation plus ultrasound and with the avalanche

method, we proceeded to test these protocols for transfection of rabbit RPE in vivo. A rabbit received a subretinal injection of  $\sim 75 \mu\text{g}$  pNBL2. Electrodes and an ultrasonic transducer were placed behind the eyeball as in Figure 1a, and the settings for electroporation plus ultrasound, as described earlier, were applied. During application, the retina became opaque in places, indicating areas of severe acute retinal damage. After 24 hours, animals were examined, and the posterior eyecups were assayed for luciferase activity. Low levels of luciferase expression were observed over a small area (Fig. 4a).

For electron avalanche transfection, two probes were constructed (see the Methods section; Fig. 4b). The probes were placed behind the sclera and aligned to the site of the bleb, and five biphasic pulses of 250  $\mu\text{s}$ /phase and  $\pm 250$  V were applied in five locations, covering the area of the subretinal bleb. Because the target RPE cells were separated from the electrodes by approximately 1 mm, the thickness of the sclera and choroid, the electric field they experienced was approximately 2.5 kV/cm. The untreated contralateral eye for each animal was used as a control. After 24 hours, treated and control eyes were enucleated, and the posterior eyecups were prepared, leaving the neural retina intact. With both probe designs, abundant luciferase activity ( $5 \times 10^6$  photons/s) was observed over the area of subretinal injection (Figs. 4c, 4d). The neural retina was removed, and luciferase activity was measured separately for the neural retina alone and the remaining eyecup. The bulk of

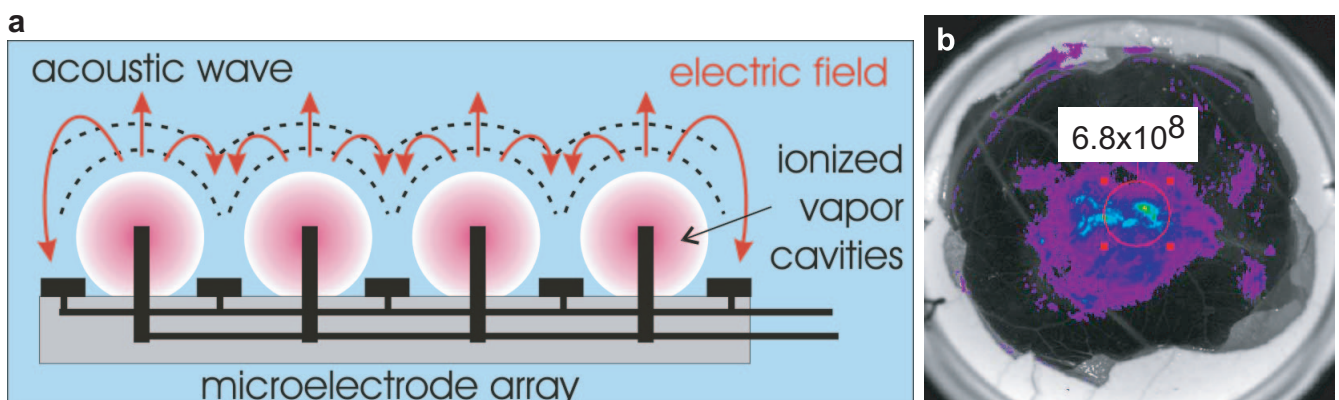
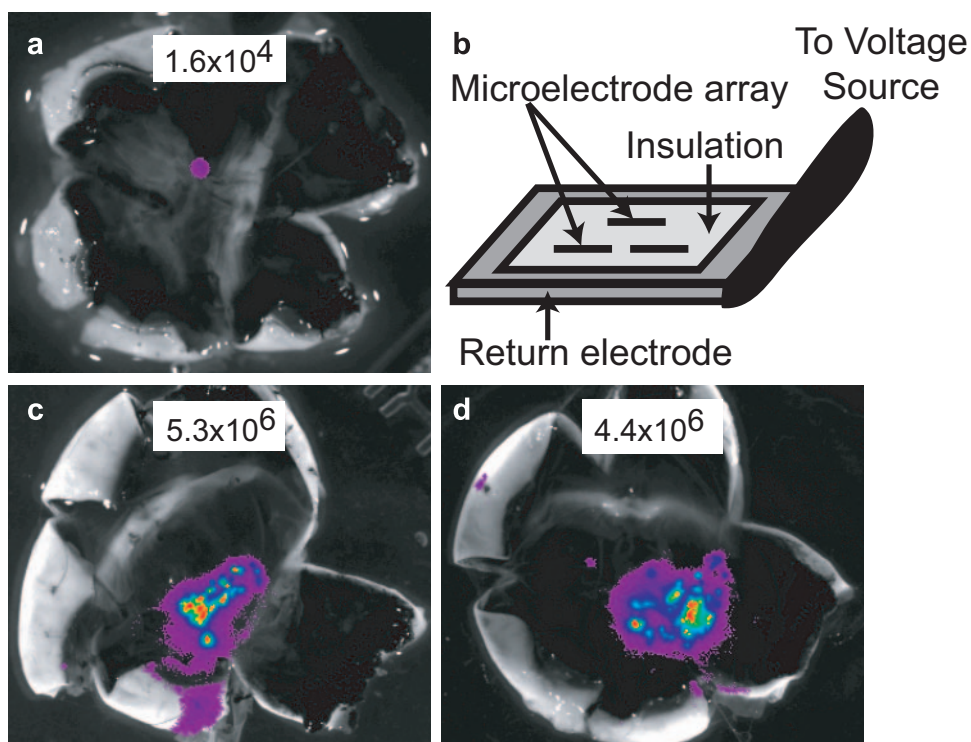


**FIGURE 3.** Electron avalanche transfection. (a) In plasma-mediated electroporation, an electronic field with high voltage amplitude is produced from microelectrodes, forming a transient vapor cavity and ionizing it, thus allowing for conductance from the electrode through the vapor cavity to the tissue (red lines). At the same time, the cavitation bubble generates a propagating acoustic wave (black lines), thus exposing the tissue to an electric field and synchronized mechanical stress. (b) Electron avalanche transfection of CAM produces higher gene expression (shown in photons/second) than electroporation plus ultrasound and much higher than electroporation alone (Fig. 2b). No marks indicating damage were visible on the tissue after treatment.

**FIGURE 4.** Application of electron avalanche transfection to rabbit RPE in vivo. (a) Optimized electroporation settings from CAM were applied along with ultrasound subsclerally after subretinal injection. After 24 hours, the eye was removed and assayed for luciferase activity. Only a small amount of transgene expression was observed. (b) A  $3 \times 3$ -mm probe designed for subsclear application of the avalanche method contained three active microelectrodes 0.05 mm in diameter and 1.5 mm in length, surrounded by a return electrode. It also included embedded fiberoptics for alignment to the subretinal bleb. (c) A rabbit was treated with electron avalanche transfection with the probe shown in (b). After 24 hours, abundant luciferase expression was observed in RPE cells in the area corresponding to the subretinal bleb. (d) A rabbit was treated with a second probe design and assayed for luciferase expression after 24 hours. Results were similar to those achieved with the first probe design. Gene expression is shown as bioluminescence measured in photons/second.



the signal was detected in the eyecup containing RPE, suggesting that the measured activity was due to DNA transfer to RPE cells rather than cells of the neural retina. Similar treatment with intravitreal administration of DNA did not yield detectable luciferase activity (data not shown).

To further investigate the retinal cell types that were transfected with the avalanche method, rabbits received pMax plasmid expressing GFP and were evaluated by in vivo fluorescence fundus photography after 48 hours. Fluorescence was strongly visible in animals treated with the avalanche method (Fig. 5a), but not when treated with injection alone (data not shown). When pMax was used, the quantity and spatial distribution of fluorescence was variable, with some experiments resulting in signal that was lower or restricted to a smaller area within the bleb. For localization of signal, frozen sections were made from treated and control eyes and evaluated by fluorescence microscopy. Transgene expression was visible in the RPE cell layer over most of the area under the bleb (Figs. 5c, 5d). In some areas, particularly around the edges of the bleb, fluorescence was also present in the outer nuclear layer of the photoreceptor cells (Fig. 5e).

### Safety of Electron Avalanche Transfection

Safety of the avalanche method was assessed in two ways: functionally with electroretinography (ERG) and structurally with histology. The full-field ERG is a panretinal measurement; therefore a wide area of the retina should be treated to observe any potentially damaging effects.

To test sensitivity of the full-field ERG, we treated one animal with long pulses that caused coagulation of the retina. Thirty spots were administered, covering more than one third of the central posterior pole. In this animal, both, the dark- and light-adapted ERG responses for the treated eye decreased by a factor of 4, to 25% of their original values and in comparison to the untreated eye (data not shown).

Three animals were then treated with similar placement of 30 spots of the treatment regimen, five biphasic pulses of 250  $\mu$ s/phase at  $\pm 250$  V. To control for the mechanical effects of

the eye manipulations, one animal was sham treated with a similar procedure, but no voltage was applied. All animals were observed by weekly ERG recordings for 4 weeks after surgery. For treated, sham-treated, and untreated animals, ERG responses were found to be within the normal range of variability<sup>32</sup> (Figs. 6a-f). After 4 weeks, the eyes were collected for histology, which also showed no difference between the treated and untreated eyes (Figs. 6g, 6h).

### DISCUSSION

This study describes a new approach for the delivery of plasmid DNA to retinal cells, including RPE and, to a limited extent, photoreceptors. We used an array of microelectrodes placed behind the eyeball to produce a localized electric field in proximity to the cells targeted for transfection, but far from the sensitive anterior structures of the eye. The approach worked well in an animal model and has potential for clinical translation, unlike previous studies that have used electrodes on the corneal surface and electroporation across the head of the animal.<sup>23,33</sup> Subretinal administration is far more effective in reaching the targeted cell types in the retina than less-invasive techniques (e.g., intravitreal injection). We acknowledge, however, that subretinal injection is more invasive and carries more clinical risk than does intravitreal injection, because a retinal detachment is necessary. We did not observe any complications associated with placing electrodes on the back of the eye, and we believe that these methods would be well tolerated by patients.

Using CAM as a model tissue, we observed that tensile stress applied by tissue stretching or by ultrasound dramatically enhanced transfection efficiency. Based on this finding we developed a new transfection method called electron avalanche transfection, which uses a high electric field to produce synchronized pulses of electric current and mechanical stress. This new method differs from conventional electroporation in several ways. First, microelectrodes are used rather than large electrodes. Second, the avalanche method relies on ionization

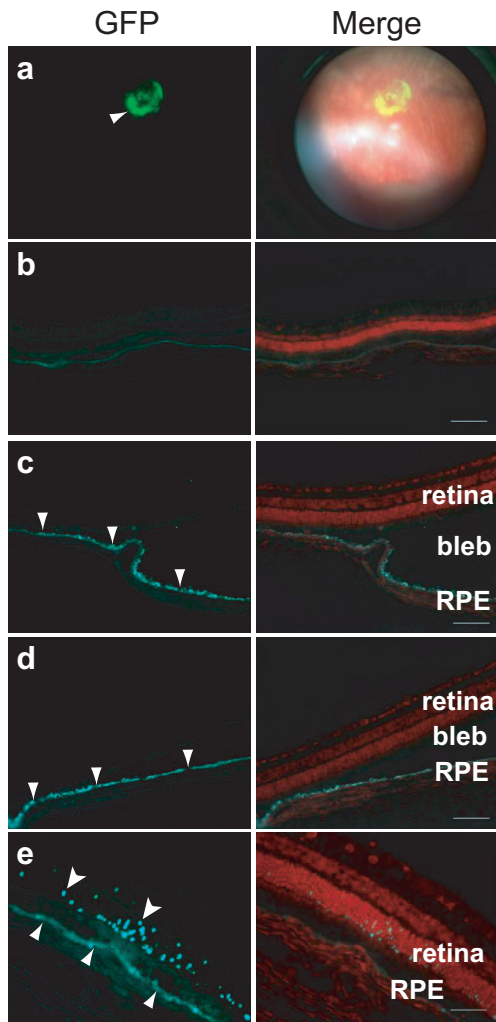


**FIGURE 5.** Localization of gene transfer in the retina after electron avalanche transfection. (a) In vivo fluorescent fundus imaging after subretinal injection plus electron avalanche transfection showed gene transfer in the retinal bleb area (*arrowhead*). (b) The untreated animal showed only background fluorescence. (c–e) Tissue from (a) was cryosectioned to identify the transfected cells. Merged reference images show propidium iodide staining to reveal retinal architecture. In the treated animal, transfected cells included RPE cells (*flat-backed arrowheads*), as well as some photoreceptor cells (*scooped-back arrowheads*).

of the vapor cavity to deliver the electric field and mechanical stress, whereas arc production is considered detrimental in conventional electroporation. These settings result in much higher electric fields: 1 to 3 kV/cm in the avalanche method, as opposed to 0.1 to 1 kV/cm with conventional settings. Third, the regimen uses pulse durations of 250  $\mu$ s per phase, whereas conventional electroporation requires pulse durations of 5 to 100 ms for efficient DNA transfer.<sup>11</sup> Because the pulse is short and biphasic, little or no muscle movement occurs when pulses are delivered, which is desirable for both precision and patient comfort. Because of these properties, electron avalanche transfection may be a preferred alternative to conventional electroporation for some applications.

An increase in efficiency of electroporation under tensile stress could occur because the lipid bilayer becomes less stable and thus more susceptible to permeabilization by the electric field. Such a hypothesis is consistent with previous work showing that membrane stretching destabilizes the lipid bilayer

and may contribute to pore formation.<sup>22</sup> It is possible that tensile stress not only reduces the threshold of electroporation, but also increases its safe dynamic range (i.e., the range of settings that cause poration but not irreversible cellular damage). The strong enhancement of permeabilization that was observed with microsecond plasma-mediated electrical discharge warrants additional studies exploring the mechanisms involved.

In the rabbit retina, conventional electroporation plus ultrasound caused severe retinal damage and did not result in efficient DNA delivery. The avalanche method, by contrast, delivered DNA efficiently, and the signal was localized predominantly to RPE cells. One reason for localized transfection could be that tight junctions between the RPE cells result in high resistance, and thus the voltage decrease across the RPE is more than across other tissue layers. In addition, cells of the neural retina were further removed from the electrodes by the subretinal bleb itself and therefore experienced lower current densities. This explanation was further supported by the observation that at the edges of the bleb, where neural retina was closer to the electrodes, some photoreceptors were also transfected. Penetration depth of the electric field into the tissue can be controlled by the geometry of the electrode array, and a different geometry may be more optimal for efficient DNA transfer to photoreceptors.

In initial experiments, the electron avalanche treatment did not cause observable damage to the retina or to anterior chamber tissues, including the lens and the cornea. Possible damage to the retina was further explored by performing ERG recordings and histology. We acknowledge, however, that the toxicity profile may be different in the presence of DNA. However, any such toxicity would be localized to the site of the injection, a relatively small area of the retina, and would therefore not be detectable by a full-field ERG. In experiments where DNA was subretinally injected and electron avalanche transfection was used, animals showed no signs of damage by fundus photography or histology. One experiment in which significantly higher settings were used for electron avalanche transfection resulted in visible damage (data not shown). In future studies, it will be important to evaluate safety over the long-term in the presence of DNA and to determine the thresholds of damage in the retina and in other tissues of interest.

One major shortcoming of nonviral DNA delivery is transient expression of the transgene. In rat RPE cells, transgene expression declines over  $\sim$ 3 weeks, probably due to gene silencing, since extrachromosomal DNA is known to persist in postmitotic tissues.<sup>23</sup> Several recent studies, however, have shown that the integrase from bacteriophage  $\phi$ C31 confers genomic integration of plasmid DNA and long-term expression in mammalian cells in a variety of contexts,<sup>23,34–40</sup> including RPE cells.<sup>23</sup> Used together, electron avalanche transfection and  $\phi$ C31 integrase would be a powerful combination for long-term, nonviral gene therapy.

Many potential applications exist for electron avalanche transfection. Although the scope of this study was limited to plasmid DNA, the method is likely to be effective for less bulky molecules as well, such as proteins, mRNA, siRNA, and small molecules. This method is amenable to a variety of cell types. In addition to efficient DNA delivery to CAM and rabbit RPE cells, we have also successfully transfected HEK293 cells *in situ* and rabbit conjunctival fibroblast explants. Follow-up experiments will test other desirable targets for gene therapy, including skeletal and cardiac muscle, liver, and skin. It is also possible to mount the microelectrode on a catheter and apply it surgically, with local injection of DNA followed by local electron avalanche transfection. Future experiments in the eye will focus on treatment of animal models of retinitis pigmentosa and age-related macular degeneration.

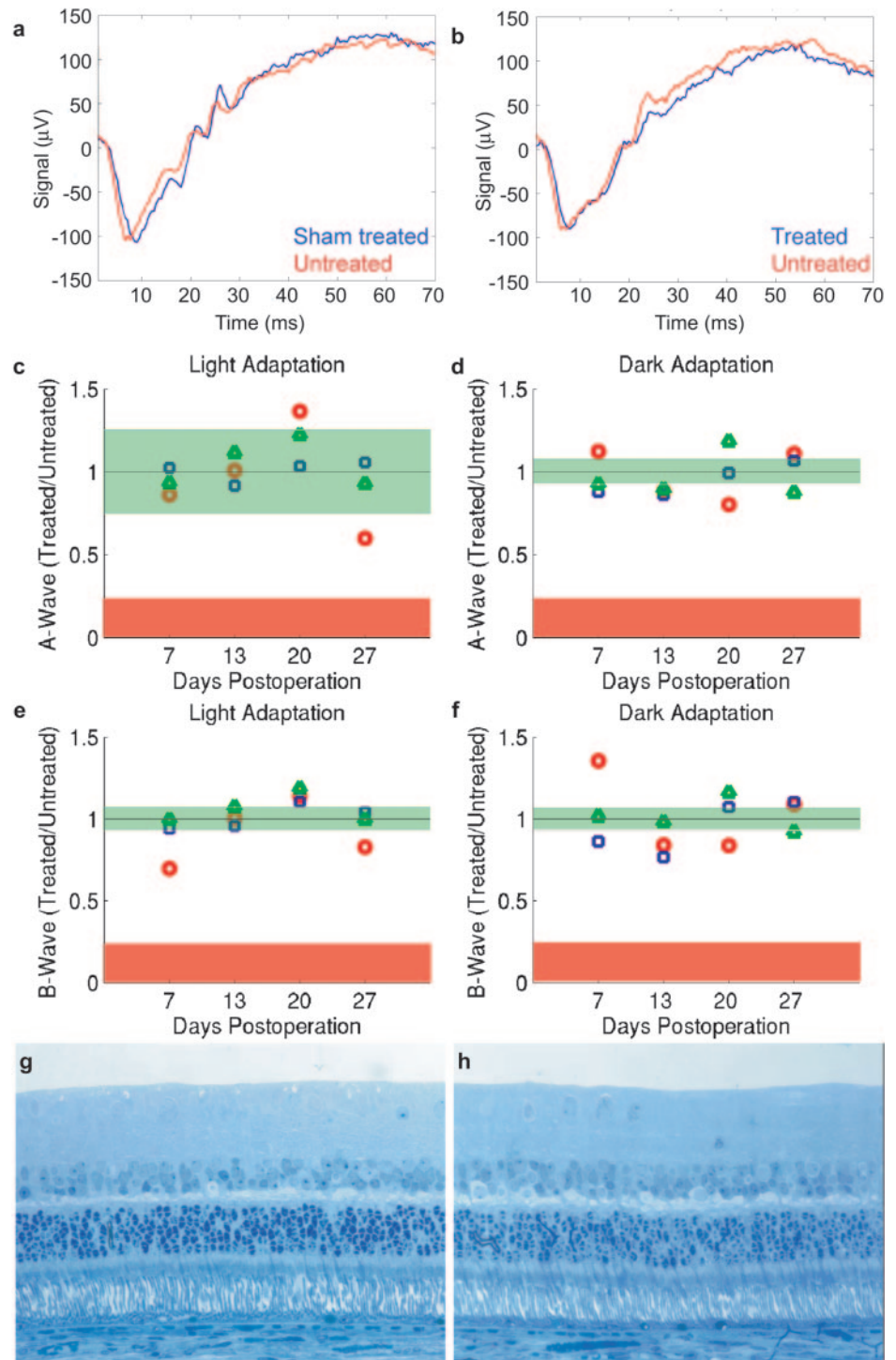


**FIGURE 6.** ERG measurements after application of the avalanche method. Animals were treated either with coagulation settings, sham treatment, or electron avalanche transfection settings over approximately one third of the central retina. (a) A dark-adapted ERG in a sham-treated animal. (b) A dark-adapted ERG in an animal treated with electron avalanche transfection shows no observed difference between the treated eye and the untreated contralateral eye. (c–f) A summary of ERG responses 4 weeks after treatment with the avalanche method are shown, including a- and b-wave amplitudes after light-adaptation and dark-adaptation. Responses are shown for the three electron-avalanche-treated animals (*circle, triangle, square*) as the ratio between treated and control eyes. *Red band*: level of significant damage, as observed in the coagulation-treated animal; *green band*: the range of experimental variation as observed in the sham-treated animal. (g) Histology from an untreated control eye. (h) Histology from an electron-avalanche-treated eye shows no difference in retinal thickness or architecture compared with the untreated control.

### Acknowledgments

The authors thank Michael F. Marmor, Mark S. Blumenkranz (both from Department of Ophthalmology, Stanford University), Robert T. Hillman (Department of Genetics, Stanford University), and Georg Schuele (Department of Ophthalmology and Hansen Experimental Physics Laboratory, Stanford University) for helpful advice and assistance.

### References

- Bennett J. Gene therapy for retinitis pigmentosa. *Curr Opin Mol Ther.* 2000;2:420–425.
- Ali RR, Sarra GM, Stephens C, et al. Restoration of photoreceptor ultrastructure and function in retinal degeneration slow mice by gene therapy. *Nat Genet.* 2000;25:306–310.
- Schlichtenbrede FC, da Cruz L, Stephens C, et al. Long-term evaluation of retinal function in Prph2Rd2/Rd2 mice following AAV-mediated gene replacement therapy. *J Gene Med.* 2003;5:757–764.
- Bennett J, Tanabe T, Sun D, et al. Photoreceptor cell rescue in retinal degeneration (rd) mice by in vivo gene therapy. *Nat Med.* 1996;2:649–654.
- Acland GM, Aguirre GD, Ray J, et al. Gene therapy restores vision in a canine model of childhood blindness. *Nat Genet.* 2001;28:92–95.

6. Narfstrom K, Bragadottir R, Redmond TM, Rakoczy PE, van Veen T, Bruun A. Functional and structural evaluation after AAV.RPE65 gene transfer in the canine model of Leber's congenital amaurosis. *Adv Exp Med Biol*. 2003;533:423-430.
7. Vollrath D, Feng W, Duncan JL, et al. Correction of the retinal dystrophy phenotype of the RCS rat by viral gene transfer of Mertk. *Proc Natl Acad Sci USA*. 2001;98:12584-12589.
8. Kootstra NA, Verma IM. Gene therapy with viral vectors. *Annu Rev Pharmacol Toxicol*. 2003;43:413-439.
9. Hacein-Bey-Abina S, Von Kalle C, Schmidt M, et al. LMO2-associated clonal T cell proliferation in two patients after gene therapy for SCID-X1. *Science*. 2003;302:415-419.
10. Nicolazzi C, Garinot M, Mignet N, Scherman D, Bessodes M. Cationic lipids for transfection. *Curr Med Chem*. 2003;10:1263-1277.
11. Andre F, Mir LM. DNA electrotransfer: its principles and an updated review of its therapeutic applications. *Gene Ther*. 2004;11(suppl 1):S33-S42.
12. Liang HD, Lu QL, Xue SA, et al. Optimisation of ultrasound-mediated gene transfer (sonoporation) in skeletal muscle cells. *Ultrasound Med Biol*. 2004;30:1523-1529.
13. Somiari S, Glasspool-Malone J, Drabick JJ, et al. Theory and in vivo application of electroporative gene delivery. *Mol Ther*. 2000;2:178-187.
14. Pliquett UF, Martin GT, Weaver JC. Kinetics of the temperature rise within human stratum corneum during electroporation and pulsed high-voltage iontophoresis. *Bioelectrochemistry*. 2002;57:65-72.
15. Lenz P, Bacot SM, Frazier-Jessen MR, Feldman GM. Nucleoporation of dendritic cells: efficient gene transfer by electroporation into human monocyte-derived dendritic cells. *FEBS Lett*. 2003;538:149-154.
16. Fechheimer M, Boylan JF, Parker S, Siskin JE, Patel GL, Zimmer SG. Transfection of mammalian cells with plasmid DNA by scrape loading and sonication loading. *Proc Natl Acad Sci USA*. 1987;84:8463-8467.
17. Guzman HR, Nguyen DX, Khan S, Prausnitz MR. Ultrasound-mediated disruption of cell membranes. I. Quantification of molecular uptake and cell viability. *J Acoust Soc Am*. 2001;110:588-596.
18. Guzman HR, Nguyen DX, Khan S, Prausnitz MR. Ultrasound-mediated disruption of cell membranes. II. Heterogeneous effects on cells. *J Acoust Soc Am*. 2001;110:597-606.
19. Miller DL, Gies RA. Enhancement of ultrasonically-induced hemolysis by perfluorocarbon-based compared to air-based echo-contrast agents. *Ultrasound Med Biol*. 1998;24:285-292.
20. Harrison GH, Balcer-Kubiczek EK, Gutierrez PL. In vitro mechanisms of chemopotentiality by tone-burst ultrasound. *Ultrasound Med Biol*. 1996;22:355-362.
21. Liu J, Lewis TN, Prausnitz MR. Non-invasive assessment and control of ultrasound-mediated membrane permeabilization. *Pharm Res*. 1998;15:918-924.
22. Tieleman DP, Leontiadou H, Mark AE, Marrink SJ. Simulation of pore formation in lipid bilayers by mechanical stress and electric fields. *J Am Chem Soc*. 2003;125:6382-6383.
23. Chalberg TW, Genise HL, Vollrath D, Calos MP. phiC31 integrase confers genomic integration and long-term transgene expression in rat retina. *Invest Ophthalmol Vis Sci*. 2005;46:2140-2146.
24. Thyagarajan B, Calos MP. Site-specific integration for high-level protein production in mammalian cells. *Methods Mol Biol*. 2005;308:99-106.
25. Marc RE, Murry RF, Fisher SK, Linberg KA, Lewis GP, Kalloniatis M. Amino acid signatures in the normal cat retina. *Invest Ophthalmol Vis Sci*. 1998;39:1685-1693.
26. Bennett J, Maguire AM, Cideciyan AV, et al. Stable transgene expression in rod photoreceptors after recombinant adeno-associated virus-mediated gene transfer to monkey retina. *Proc Natl Acad Sci USA*. 1999;96:9920-9925.
27. Leng T, Miller JM, Bilbao KV, Palanker DV, Huie P, Blumenkranz MS. The chick chorioallantoic membrane as a model tissue for surgical retinal research and simulation. *Retina*. 2004;24:427-434.
28. Miller JM, Palanker DV, Vankov A, Marmor MF, Blumenkranz MS. Precision and safety of the pulsed electron avalanche knife in vitreoretinal surgery. *Arch Ophthalmol*. 2003;121:871-877.
29. Palanker D, Vankov A, Bilbao K, Marmor M, Blumenkranz M. Optimization of the pulsed electron avalanche knife for anterior segment surgery. *Proc SPIE*. 2003;4951:56-61.
30. Palanker DV, Marmor MF, Branco A, et al. Effects of the pulsed electron avalanche knife on retinal tissue. *Arch Ophthalmol*. 2002;120:636-640.
31. Palanker DV, Miller JM, Marmor MF, Sanislo SR, Huie P, Blumenkranz MS. Pulsed electron avalanche knife (PEAK) for intraocular surgery. *Invest Ophthalmol Vis Sci*. 2001;42:2673-2678.
32. Gyorloff K, Andreasson S, Ehinger B. Standardized full-field electroretinography in rabbits. *Doc Ophthalmol*. 2004;109:163-168.
33. Matsuda T, Cepko CL. Electroporation and RNA interference in the rodent retina in vivo and in vitro. *Proc Natl Acad Sci USA*. 2004;101:16-22.
34. Thyagarajan B, Olivares EC, Hollis RP, Ginsburg DS, Calos MP. Site-specific genomic integration in mammalian cells mediated by phage phiC31 integrase. *Mol Cell Biol*. 2001;21:3926-3934.
35. Olivares EC, Hollis RP, Chalberg TW, Meuse L, Kay MA, Calos MP. Site-specific genomic integration produces therapeutic Factor IX levels in mice. *Nat Biotechnol*. 2002;20:1124-1128.
36. Ortiz-Urda S, Thyagarajan B, Keene DR, et al. Stable nonviral genetic correction of inherited human skin disease. *Nat Med*. 2002;8:1166-1170.
37. Ortiz-Urda S, Thyagarajan B, Keene DR, Lin Q, Calos MP, Khavari PA. PhiC31 integrase-mediated nonviral genetic correction of junctional epidermolysis bullosa. *Hum Gene Ther*. 2003;14:923-928.
38. Quenneville SP, Chapdelaine P, Rousseau J, et al. Nucleofection of muscle-derived stem cells and myoblasts with phiC31 integrase: stable expression of a full-length-dystrophin fusion gene by human myoblasts. *Mol Ther*. 2004;10:679-687.
39. Hollis RP, Stoll SM, Scimmenti CR, Lin J, Chen-Tsai Y, Calos MP. Phage integrases for the construction and manipulation of transgenic mammals. *Reprod Biol Endocrinol*. 2003;1:79-89.
40. Groth AC, Fish M, Nusse R, Calos MP. Construction of transgenic *Drosophila* by using the site-specific integrase from phage phiC31. *Genetics*. 2004;166:1775-1782.